Journal of Inventive Engineering and Technology (JIET)
ISSN: 2705-3865
Volume-2, Issue-3, pp-19-39
www.jiengtech.com
Research Paper Open Access

COMPOSITE RESPONSE COMPARATIVE ANALYSIS, MODELLING, VALIDATIONS, AND REGRESSORS EFFECTS ON RAMIE FIBRE REINFORCED POLYESTER MATERIAL STRENGTH PROPERTIES

[1](**George O. Okoronkwo,** Department of Chemical Engineering, Micheal Okpara University of Agriculture, Umudike, Abia State, Nigeria) okoronkwo.george@mouau.edu.ng

[2](**Ibe Kizito Chidozie,** Department of Civil Engineering, Micheal Okpara University of Agriculture, Umudike, Abia State, Nigeria) ibe.kizito@mouau.edu.ng

[3](**Simeon I. Bright,** Department of Mechanical Engineering, Micheal Okpara University of Agriculture, Umudike, Abia State, Nigeria) simeonbright@mouau.edu.ng

Corresponding Author: ogeorgeonyeka@gmail.com

ABSTRACT : *The study is undertaken to find the composite response comparative analysis, modelling, validations, and regress-ors' effects on ramie fibre reinforced polyester material strength properties. For this purpose ramie fibre of aspect ratio $\left(\frac{l}{d}\right)$ as 16.67, 50.00 and 83.33 were used. Samples were casted by using nine different sample mixtures with 10 % 20 % and 30 % ramie fibres by volume of polyester. At the end of curing these casted samples were subjected to material strength tests like compressive strength, split tensile strength, flexural strength and ultrasonic pulse speed test. The control polyester composite materials compressive strength, split tensile strength, flexural strength and average ultrasonic pulse velocity are 44.0 MPa, 2.6 MPa, 4.6 MPa and 4531 m/s. The ramie fibre aspect ratios of 16.67, 50.00 and 83.33 possess compressive strength of 48.2 MPa, 54.81 MPa and 58.68 MPa, split tensile strength of 3.1 MPa, 3.89 MPa and 5.00 MPa, flexural strength of 5.6 MPa, 7.42 MPa and 9.05 MPa and average pulse velocity of 4700 m/s, 4875.25 m/s and 5870.65 m/s, respectively. Compressive strength improved by 9.55 to 33.36 %, split tensile strength enhancements of 19.23 to 92.31 %, flexural strength increased by 21.74 to 96.74 % and average ultrasonic pulse velocity improved by 3.73 to 29.57 %. Also, from strength properties models it is found that the ramie fibre polyester polymer composites has optimum compressive strength, split tensile strength, flexural strength and average ultrasonic pulse velocity of 58.03 MPa, 5.033 MPa, 9.237 MPa at 95 % adequacies and 5694 m/sec below 95 % adequacies with 66.66, 83.33, 76.66 and 83.33 optimum fibre aspect ratios and 32, 36, 36 and 50 optimum fibre volume fractions at 91.53 %, 99.39 %, 97.66 % and 81.93 % accuracies all at 1.8500, 0.0067, 0.0918 and 5.5369e+04 mean square errors. It was observed that ramie fibre along with polyester mixture has significantly improved these properties. Regression analysis on experimental results generated some statistical model predicting the results in good agreement.*

KEYWORDS: *Composite response comparative analysis; Compressive strength; Flexural strength; Split tensile strength; Ultrasonic pulse velocity; Modelling; Validations; Regressors effects*

Date of Submission: 04-12-2022 Date of acceptance: 10-12-2022

I. INTRODUCTION

Recently due to environmental concerns and the need for high-performance engineered materials the demand for industries to employ green composites material had risen reported by (Ezeokupe et al., 2021). They had also become the yard stick of recent investigations of eco-friendly and sustainable natural fibre reinforced polymer composites (NFPC's) developments rather than synthetic once. In the case of building materials fire-retardant properties requirements polymer composites with phenolic based glass fibre were prominent reported by (Ferdous et al.,2018) and (Madu et al.,2019). For eco-friendly satisfactions, natural fibre reinforcements obtained from plants, animals and bio waste may be of better choice. In the recent times, bio waste fibres have been the key needs for researchers due to quest for sustainable resources. Examples of bio waste fibres are oil palm, bagasse, corn, stalks, coir, bamboo, pineapple, banana, rice husk and ramie. These fibres are normally obtained by retting processes from any part of the plant such as stem, leaf, seed or fruit reported by (Dungani et al. 2016). Natural fibre polymer composites (NFPCs) are strain rates sensitive because its matrix viscoelastic nature. Put properly, natural fibre polymer composites (NFPCs) mechanical properties are highly dependent on the strain rates as reported by (Othman et al. 2016) and (Madu et al. 2020). Strain rates are the rates of change of strain or measures of deformation per unit second (). These rates have wide application in common engineering structures with levels ranging from low to very high rates. For example, low strain rates (< 0.1) have application in materials' creep, quasi-static deformation of structures, vehicle impacts, some parts of plane crash and earthquake or wind-induced dynamic motion of high-rise building reported by (Othman et al. 2016). While for high strain rates (> 0.1), there are applications such as armour penetration, crashworthiness of materials, blast, hard impacts from plane crash, missile and rock falls investigated by (Othman et al. 2016). Despite engineering structures, manufacturing processes are also involved with strain rates. For example, material forming, high-speed machining, potential application of super-plastic forming and diffusion bonding with automatic control manufacturing system reported by (Othman et al. 2016). In similar fashion with any other viscoelastic materials, natural fibre polymer composites (NFPCs) properties e.g., the stress–strain behaviour, failure mechanism and failure probability are distinctive under different ranges of strain rates. The mechanisms of natural fibre polymer composites (NFPCs) under various strain rates had been investigated. For example, (Kumar et al. 2019) studied coir particle interaction with epoxy polymer composites subjected to low tensile strain rates of 1 to 3 mm/min. The crack initiation and propagation in the tensile tests were observed to be extremely affected by the strain rate variation. (Siva et al. 2019) studied and observed that the cork powder reinforced with epoxy polymer composite bending stress and strain are also sensitive when subjected to a wide range of strain rates.

In any composite material both the reinforcements and matrix materials play a crucial role as reported by (Ezeokpube et al. 2018). The reinforcement materials behave as the load-carrier whereas the matrix materials behave as the load-distributer when the composite is subjected to an external load reported by (Sanjay et al. 2018). The matrix materials are classified as either thermo-set polymers or thermoplastic polymers (Okoronkwo et al. 2019). Thermoplastic materials can be reused after the curing process at proper treatment heat conditions. Some examples of thermoplastic polymers are polyester, polypropylene, nylon, and Teflon. Unlike thermoplastic polymers, thermo-set polymers cannot be reused after the curing process. For a required temperature, once thermo-set condensed (solidified) it cannot be recycled. The most common thermo-set resins are epoxies, unsaturated polyesters, polyamides, and vinyl esters studied and reported by (Okoronkwo et al. 2019). Recently, thermo-set materials have become more popular than thermoplastic materials due to their wide range of applications in various sectors reported by (Messana et al. 2017) and (Madu et al. 2019). Among all polymer composites, thermo-set polymers based on epoxy resin composites have had the most attention due to their good adhesive properties, low contraction, curing (liquid-state to solid-state) time, and ease of use studied and reported by (Messana et al. 2017). Although chemical composition of natural fibres plays a good role in natural plant fiber composites, but climatic dissimilarity and geographical changes as an environmental conditions influence the composition of natural fibres. In general natural plant fibres are composed mainly of cellulose, hemi-cellulose, and lignin as reported by (Madu et al. 2018). Cellulose content and the aspect ratio of natural fibres play a key role in mechanical performance reported by (Wang et al. 2019). The mechanical properties of artificial (synthetic) fibres do not change much even with the absent of these chemical compositions. On the other hand, natural fibres grow in open environments with the assistance of air, light, water, soil, etc. These conditions vary from time to time, which affects the properties of the fibres as studied and reported by (Chokshi et al. 2020) and (Riccio et al. 2018). Some research studies have been conducted and observed that fibre composites reinforced with high cellulose-rich natural plant fibres like ramie, hemp, flax, banana, etc., have superior properties to composites reinforced with natural fibres with lower cellulose content reported by (Karimah et al. 2021) and (Madu et al. 2018).

Numerous researchers working with natural fibre composites in the presence of thermo-set materials have shown interest. Moisture uptake and flame-retardancy properties still limit the applications natural fibre composites, although there are many advantages reported by (Madu et al. 2018). (Neves et al. 2020) investigated the mechanical properties of hemp fibre composites with various matrix materials. They made a comparison between epoxy and polyester polymers. They observed that hemp fibre composites reinforced epoxy polymer have superior properties than polyester polymer composites and stated that these composites have a potential uses in armed applications. (Sapuan et al. 2019) investigated the mechanical properties of woven banana-fibre-reinforced epoxy composites. They developed theoretical model based on the ANOVA technique to compare the experimental results. Then, they observed that there was a slight variation in the theoretical and experimental results. Numerous researchers have offered useful and comprehensive review articles on natural-fibre-reinforced hybrid composites and mechanical performance importance as reported by (Mochane et al. 2019), (Sharavanan et al. 2018) and (Abedom et al. 2021). (Alhazmi et al. 2021) worked on tribological and mechanical properties of hybrid composites reinforced with epoxy polymer. They observed that the presence of nano-filler materials cannot affect any sort of improvement made in terms of wear resistance of the composite material. (Alhazmi et al. 2021) studied the mechanical properties of flax fibres subjected to various environmental conditions. They also observed that mechanical properties that were measured experimentally agreed strongly with the statistical results obtained.'

In the present study, unsaturated polyester polymer was used as binder in the production of ramie fibre polyester polymer composite. The strength properties and material characteristics of ramie fibre polyester polymer composite containing various ramie fibre aspect rations and volume fractions were conducted.
The aim of this study was to study composite response comparative analysis, modelling, validations, and regress-ors' effects on ramie fibre reinforced polyester material strength properties were carried out.
The novelty of this research cuts across the introduction of a new plant fibre and a new polymer composite material with a new locally sourced plant stem fibre possessing dual functions (i.e., functions as both reinforcement/filler materials for the composite industries and fabrics for the textile industries) to structural and material engineers and the general public as a whole. Thereby reducing the undesirable costs and fatigues associated with the quest for a reinforcement/doping/filler material that must increases the strength properties of the ramie fibre polyester polymer composite (RFPPC) under investigation. By this research also the indigenous people of Nekede in Imo State, Nigeria, from where the reinforcement were sourced from and the world as well will be exposed to a new advanced but highly economical engineered natural fibre reinforced polyester polymer composite (i.e., RFPPC). That will provide jobs to them, revenue to both Imo State and Nigerian governments, entire Nigerian populace in general and the world at large.

The structure of this paper is as follows: in section II, the raw materials are presented. Next, mixture design and preparation of samples followed by response surface methodology, experimental design, statistical analysis and mathematical model development to ascertain the needed regression model with number of ramie fibre polyester polymer composite samples with respect to estimated responses and independent variables and their analysis of variance. Then, experimental methods to determine compressive strengths split tensile strengths, flexural strength and ultrasonic pulse velocity. In section III, presentations of the results obtained are provided. Next, regression models employed to model the experimental results obtained were presented as experimentally validated. While discussions of the results obtained are provided in section III B. A response methodology model of the ramie fibre polyester polymer composite proposed and established in the previous sections was employed and results presented in section III were discussed. The optimum conditions, surface plots and response functions obtained from the proposed model are compared and, subsequently, experimentally validated. Section IV contains the final conclusions that summarize the most important achievements of this article.

II. MATERIALS AND METHODS

A. MATERIALS

These were as depicted as follow:

Ramie fibres with different lengths were obtained from ramie stem extracted from the ramie plant obtained from local forest in Nekede, Owerri, Imo State, Ngeria. Catalyst, hardener and unsaturated polyester resin with density 1.40 g/cc, were supplied by Nycil Company Limited, Nigeria.
In the current research ramie fibre was the reinforcement, unsaturated polyester resin the matrix material, cobalt nephthanate the curing agent and the catalyst was methyl ethyl ketone peroxide. Unsaturated polyester resins are

always unsaturated synthetic polymers produced when polyhydric alcohols comes in contact with dibasic organic acids. The most common employed raw material is maleic anhydride possessing di-acid functional group. Unsaturated polyester the outcome of condensation polymers produced when polyhydric alcohols, reacts with organic compounds with multiple hydroxyl functional groups producing saturated or unsaturated dibasic acids. The properties of ramie and unsaturated polyester resin are depicted in Tables 1 and 2, respectively,

Table 1: Physical and strength properties of ramie fibre

Diameter (μm)	Density (g/cc)	Tensile modulus (GPa)	Tensile strength (MPa)	Elongation at yield (%)
100.00-300.00	1.20	5.00	175.00	15.00

Table 2: Physical and strength properties of unsaturated polyester resin

Matrix	Melt flow index (g/10 min)	Density (g/cc)	Tensile modulus (GPa)	Tensile strength (MPa)	Elongation at yield (%)
UPR	11.00	1.40	1.47	36.00	10.00

(a)

(b)

(c)

(d)

Fig.1: Images of the (a) Ramie fibre and some ramie fibre polyester composite samples; (b) unsaturated polyester resin; (c) Initiator/Accelerator; (d) Catalyst;

B. RESPONSE SURFACE METHODOLOGY, EXPERIMENTAL DESIGN, STATISTICAL ANALYTIC TECHNIQUES AND MATHEMATICAL MODEL DEVELOPMENT

Response surface methodology (RSM) one of the most accepted optimization techniques for optimizing the variable conditions before the production of the unsaturated polyester polymer composites. The experimental design was conducted by the use of MATLAB R2007b (Math Works, Inc.). By the application of central composite design (CCD), two independent variables were considered in three steps: conducting the test designed properly, predicting the mathematical model coefficients, and examining the model validation. Below is the depicted mathematical model:

$$Y = f(C_1, C_2, C_3, ...C_n) + \varepsilon \quad (2.1)$$

where Y represents responses, C represents dependent variables, n represent variables number under investigation, while error is donated by ε. A second order can depict the effect of parameters in linear, quadratic, and cross product terms. The variables used were fibre aspect ratio (c_1) and fibre volume fraction (c_2). Certain numbers of tests are required to be conducted according to CCD: $2n$ axial experiments, 2^n at the centre, and n_c

replicates in centre point. The response functions measured were tensile strengths and tensile modulus. An n^{th}-order polynomial model can study the influence of parameters under linear, quadratic, and cross product conditions, being the function of variable x, was plotted for each variable as shown below (Madu et al. 2018):

$$Y = \beta_0 + \sum_{i=1}^{n} \beta_i c_i + \sum_{i=1}^{n} \beta_{ii} c_i^2 + \sum_{i<j}^{n} \sum_{j}^{n} \beta_{ij} c_i c_j + \varepsilon \qquad (2.2)$$

where Y is the estimated responses; β_0, a_i, β_{ii}, β_{ij} and ε are constants (β_0 is constant term, β_i are the constant coefficients of linear terms, β_{ii} are the constant coefficients of quadratic terms, while β_{ij} is the constant coefficients of interactive terms) and ε is the constant error components; and c_1, and c_2 are the coded values of the regressor variables representing fiber aspect ratios and fiber volume fractions, respectively. In each factor was the variance divided into say linear, quadratic, and interaction terms. The suitability of the n^{th}-order polynomial model and the significance of these variables were determined with lack-of-fit and error components.

The effects of the considerable parameters on the process were determined by ANOVA. To check further for parameters significance P and F values were used. As a lower P value affects the process enormously the P (probability) value comes in when data samples were subjected to null hypothesis. On the opposite, null hypothesis are rejected by data samples with large F values but samples with higher F values are expected to be significant.

Levels of process variables were obtained with CCD model. Two-process variable 2^2 CCD model was developed as seen earlier (Madu et al. 2018). This model contained 9 sets of experiments as seen in equation (2.3)

$$N = 2^n + 2n + n_c = 2^2 + 2 * 2 + 1 = 9 \qquad (2.3)$$

C. METHODS

This section cover the methods of research.

a. Experimental production of ramie-polyester composite materials

The composites were reinforced with ramie fiber reinforcement in UPR matrix material. The uniformly agitated fibres with unsaturated polyester resin were emptied in the mould and placed in compression moulding machine. Manufacturing of samples was performed by utilizing manually operated and temperature regulated compression moulding machine. The knotted fibres were obtained from ramie plant and were cleaned up. These fibres were passed through a Knot Separating Machine to evacuate the bunch and to separate individual fibres. The fibres acquired from bunch isolating machine are dried in daylight for a time period of 48 hrs to remove the moisture. Fibres were cut to different lengths (10 mm – 50 mm) with 0.6mm diameter to be utilized for randomly oriented fibre mats. In this process, the spacers were utilized for casting composite boards of size 300 mm x 300 mm x 4 mm thicknesses. These were placed on the base plate and a thick mylar (a non sticky) sheet is placed in between spacers and base plate for the easy removal of composite samples after curing (Madu et al. 2018).

Polymer (unsaturated polyester), catalyst (methyl ethyl ketone peroxide) and hardener (cobalt naphthanate) were mixed in a proportion of 50:1:1 i.e., 1000 ml: 20 ml: 20 ml in ratio and stirred to uniform compositions. Different lengths of ramie fibre of different required fibre volume fractions (i.e., 10 %, 30 % and 50 % for 10 mm; 10 %, 30 % and 50 % for 30 mm; 10 %, 30 %, and 50 % for 50 mm, respectively) were weighed and distributed uniformly at the bottom of the mould inside the spacers. Compression load was then applied for 15 minutes on mould containing the fibres. Resin was then applied uniformly on fibres. Another releasing mylar sheet is spread over at the top surface with a steel plate and then the sample was compressed for one hour for uniform distribution of matrix and elimination of entrapped air bubble if any. Here the temperatures of both base plates were maintained at ambient conditions. The composite samples were cut from the casted composite panels. The tensile, flexural, compressive, impact and ultrasonic pulse velocity tests of every sample in the current study was determined according to ASTM D638 for split tensile strength, ASM D 790 for flexural strength, ASTM D...for compressive strength, ASTM D...impact strength and ASTM D...for ultrasonic pulse velocity tests standards. The sizes of testing samples were considered as 100 mm x 20 mm x 't', where 't' is the thickness of samples kept constant at 4 mm.

b. Casted ramie-polyester composite strength properties characterization

This section covers the sub-topic as follows.

c. Compressive strength test

The mixtures were prepared according to the procedure given in previous sections, and were casted in 40 mm cubic mould and left to harden at room temperature. At the end of curing in room temperature, the samples were tested for compressive strengths. Compressive strengths were carried out and tested according to ASTM C 579-01 Method B. Tested by using a Gilson universal compression testing machine of 2000 Kn maximum capacity at 2.2 Kn/sec. Loading rate, produced by Gilson company, USA. The compressive strength was determined as the quotient of the maximum compressive force and the cross-sectional area of the sample according to the equation (2.4):

$$R_c = \frac{F_{cmax}}{A} \tag{2.4}$$

where: R_c – compressive strength $[N/mm^2]$, F_{cmax} – maximal compressive force [N], A – the sample's cross-sectional area $[mm^2]$.

d. Split tensile strength test

Tensile tests were performed on casted samples according to ASTM test standard D 638 with the help of universal testing machine MCS NE-20. The samples specifications as per standard and actual samples configurations were followed. The tensile strength was determined as the quotient of the maximum tensile force with the cross-sectional area of the sample according to the equation (2.5) (Okoronkwo et al.2016):

$$R_t = \frac{F_{tmax}}{A} \tag{2.5}$$

where: R_t – Split tensile strength $[N/mm^2]$, F_{tmax} – maximal tensile force [N], A – the sample's cross-sectional area $[mm^2]$.

e. Flexural strength

Testing the flexural strength of the ramie fibre composite material refers to standard ASTM D 790. The flexural strength was measured using universal testing machine (UTM) Exceed Model E43. Dimensions, gauge length and cross-head speed were selected according to standard ASTM D-790 at a cross head speed of 0.8 mm / min and a gauge length of 25 mm. The flexural strength was determined as the quotient of the maximum tensile force with the cross-sectional area of the sample according to the equation (2.6) (Onukwuli et al. 2016):

$$FSL_t = \frac{3P_{tmax}L}{2bt^2} \tag{2.6}$$

where: FSL_t – flexural strength $[N/mm^2]$, P_{tmax} – maximal flexural force [N], b – the samples breath [mm]. t – the samples thickness [mm], and L – the samples span length [mm].

f. Ultrasonic pulse Velocity

At present, the pulse velocity method is used for ramie composite testing. This method enables the evaluation of ramie composite strength and homogeneity. In a limited range, the ultrasonic pulse velocity method is also applied for determination of the elasticity constants, detection of crack geometry [J.Kaszyński, 2000], and evaluation of the degree of ramie composite degradation.

III. RESULTS AND DISCUSSION

This section presents the results and discussion.

Table 1: Strength properties table for ramie fibre reinforced polyester composite mixtures

Composite Strength properties	Run number	Residuals	Predicted values (MPa)	Actual values (MPa)	Percentage increase (%)
Compressive strength	1	0.0000	0.00	44.00	0.00
	2	-0.4011	48.60	48.20	9.55
	3	0.2122	52.19	52.40	19.09
	4	0.1889	53.45	53.64	21.91
	5	1.2489	53.56	54.81	24.57
	6	-1.3178	56.74	55.42	25.96
	7	0.0689	56.09	56.16	27.64
	8	-0.8478	54.57	53.72	22.09
	9	1.1056	53.17	54.28	23.36
	10	-0.2578	58.94	58.68	33.36
Split tensile strength	1	0.0000	0.00	2.6	0.00
	2	-0.0567	3.16	3.1	19.23
	3	-0.0500	3.65	3.6	38.46
	4	-0.0067	3.69	3.68	41.54
	5	-0.0900	3.98	3.89	49.62
	6	0.0533	4.47	4.52	73.85
	7	0.0367	4.65	4.69	80.39
	8	0.0333	4.38	4.41	69.62
	9	-0.0033	4.79	4.79	84.23
	10	-0.0300	5.03	5.00	92.31
Flexural strength	1	0.0000	0.00	4.60	0.00
	2	0.0028	5.59	5.60	21.74
	3	-0.2056	6.81	6.60	43.48
	4	0.2028	6.51	6.71	45.87
	5	0.0778	7.34	7.42	61.30
	6	0.2444	7.78	8.02	74.35
	7	-0.3222	9.32	9.00	95.65
	8	-0.0806	7.56	7.48	62.61
	9	-0.0389	8.94	8.90	93.48
	10	0.1194	8.93	9.05	96.74
Ultrasonic pulse Velocity	1	0.0000	0.00	4531.00	0.00
	2	-1.7618	4701.76	4700.00	3.73
	3	0.9100	4868.09	4869.00	7.46
	4	-0.0541	4875.30	4875.25	7.59
	5	0.5399	4893.80	4894.34	8.02
	6	0.3930	4953.22	4953.61	9.33
	7	-1.1305	5074.08	5072.95	11.96
	8	0.3507	4888.67	4889.02	7.90
	9	-1.9455	4912.95	4911.00	8.39
	10	0.4054	5870.19	5870.60	29.57

Table 2: Analysis of variance table for ramie fibre polyester Composite strength properties

Composite Strength properties	Source	Sum Sq.	d. f.	Mean Sq.	F	Prob>F
Compressive strength	C1 C2 C3 Error Total	33.6067 23.0671 8.8624 65.5362	2 2 4 8	16.8033 11.5335 2.2156	7.58 5.21	0.0435 0.077
Split tensile strength	C1 C2 C3 Error Total	2.57787 0.70807 0.02367 3.3096	2 2 4 8	1.28893 0.35403 0.00592	217.85 59.84	0.0001 0.001
Flexural strength	C1 C2 C3 Error Total	8.2201 3.2168 0.3194 11.7563	2 2 4 8	4.11004 1.60841 0.07984	51.48 20.14	0.0014 0.0082
Ultrasonic pulse velocity	C1 C2 C3 Error Total	254828.5 335989.4 328669.9 919487.8	2 2 4 8	127414.2 167994.7 82167.5	1.55 2.04	0.3173 0.2445

Table 3: Response Surface Model based on ramie fiber polyester composite strength properties

Composite Strength properties	VARIABLES	Coefficients	Std. Error	t-stat	P-value	F-stat
Compressive strength	Constant C1 C2 C1 * C2 C1.^2 C2.^2	39.7300 0.2811 0.5663 -0.0014 -0.0018 -0.0078 R^2 = 0.9153	2.9282 0.0933 0.1555 0.0010 0.0009 0.0024 AdjR^2 = 0.7742	13.5680 3.0120 3.6411 -1.3381 -2.0552 -3.1418 Mse = 1.8500	0.0009 0.0571 0.0357 0.2733 0.1321 0.0516 CV =	sse = 5.55 dfe = 3 dfr = 5 ssr = 59.986 f = 6.4849 pval = 0.077396
Split tensile strength	Constant C1 C2 C1 * C2 C1.^2 C2.^2	1.7177 0.0448 0.0756 -4.5005e-005 -0.0002 -0.0010 R^2 = 0.9939	0.1761 0.0056 0.0094 6.1345e-005 5.2058e-005 0.0001 AdjR^2 = 0.9838	9.7557 7.9756 8.0828 -0.7336 -4.6688 -7.0031 Mse =0.0067	0.0023 0.0041 0.0039 0.5163 0.0186 0.0059 CV =	sse = 0.020067 dfe = 3 dfr = 5 ssr = 3.2895 f = 98.358 pval = 0.0015942
Flexural trengsth	Constant C1 C2 C1 * C2 C1.^2 C2.^2	2.8426 0.0957 0.1551 0.0002 -0.0007 -0.0023 R^2 = 0.9766	0.6521 0.0208 0.0346 0.0002 0.0002 0.0005 AdjR^2 = 0.9376	4.3589 4.6039 4.4788 0.6933 -3.5170 -4.2874 Mse = 0.0918	0.0223 0.0193 0.0208 0.5380 0.0390 0.0233 CV =	sse = 0.27528 dfe = 3 dfr = 5 ssr = 11.481 f = 25.024 pval =0.01191
Ultrasonic pulse Velocity	Constant C1 C2 C1 * C2 C1.^2 C2.^2	5109.500 -7.0376 -24.8670 0.3024 0.0409 0.3479 R^2 = 0.8193	506.5800 16.1460 26.9050 0.1765 0.1498 0.4159 AdjR^2 = 0.5183	10.0860 -0.4359 -0.9243 1.7135 0.2736 0.8364 Mse = 5.5369e+04	0.0021 0.6924 0.4235 0.1851 0.8022 0.4643 CV =	sse = 1.661e+005 dfe = 3 dfr = 5 ssr = 7.5338e+005 f = 2.7213 pval =0.21972

a. Ramie fibre polyester composite compressive strength

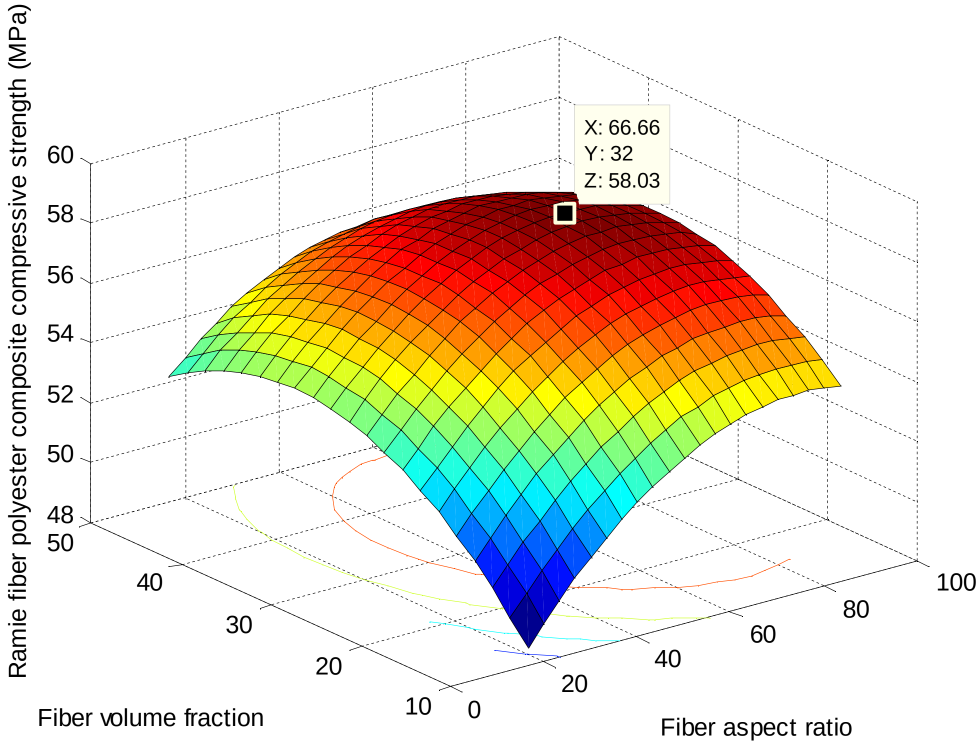

Fig.2: Surface plot for ramie fiber polyester Composite compressive strength

b. Optimization of ramie fiber polyester Composite compressive strength

Optimization terminated: magnitude of directional derivative in search direction less than 2*options. TolFun and maximum constraint violation is less than options. TolCon.
No active inequalities.
x = 66.9341 31.4316
fval = -58.0365

c. **Ramie fibre polyester composite split tensile strength**

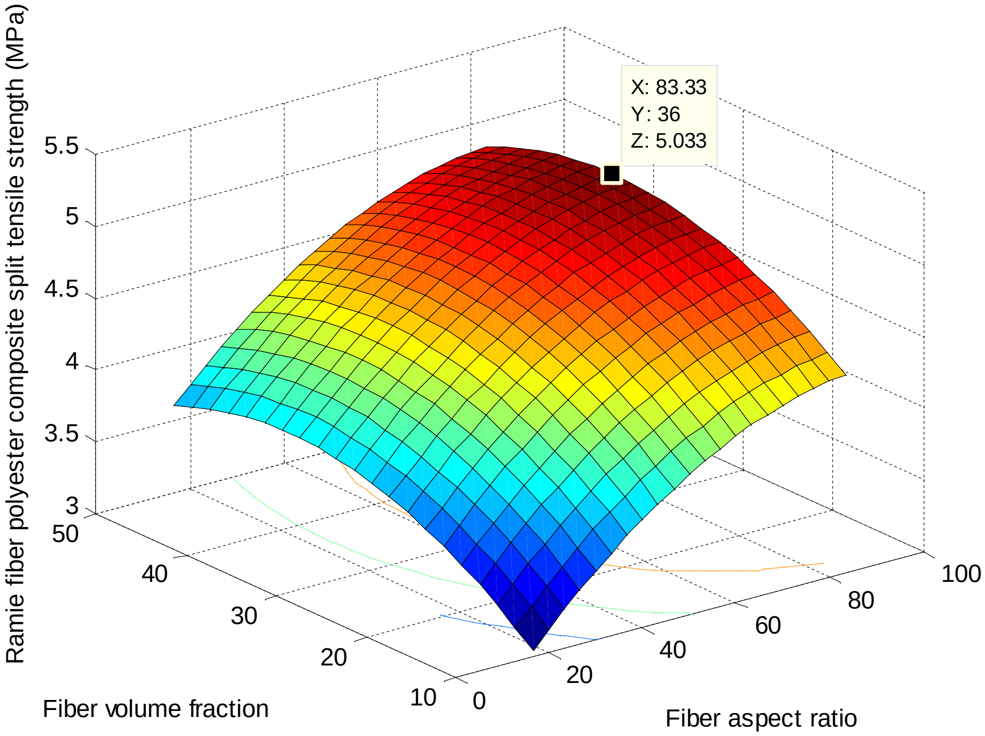

Fig.3: Surface plot for ramie fiber polyester Composite split tensile strength

d. **Optimization of ramie fiber polyester Composite split tensile strength**

Optimization terminated: first-order optimality measure less than options. TolFun and maximum constraint violation is less than options. TolCon.

Active inequalities (to within options. TolCon = 1e-006):

lower upper ineqlin ineqnonlin

1

x = 83.3300 35.4734

fval = -5.0337

e Ramie fibre polyester composite flexural strength

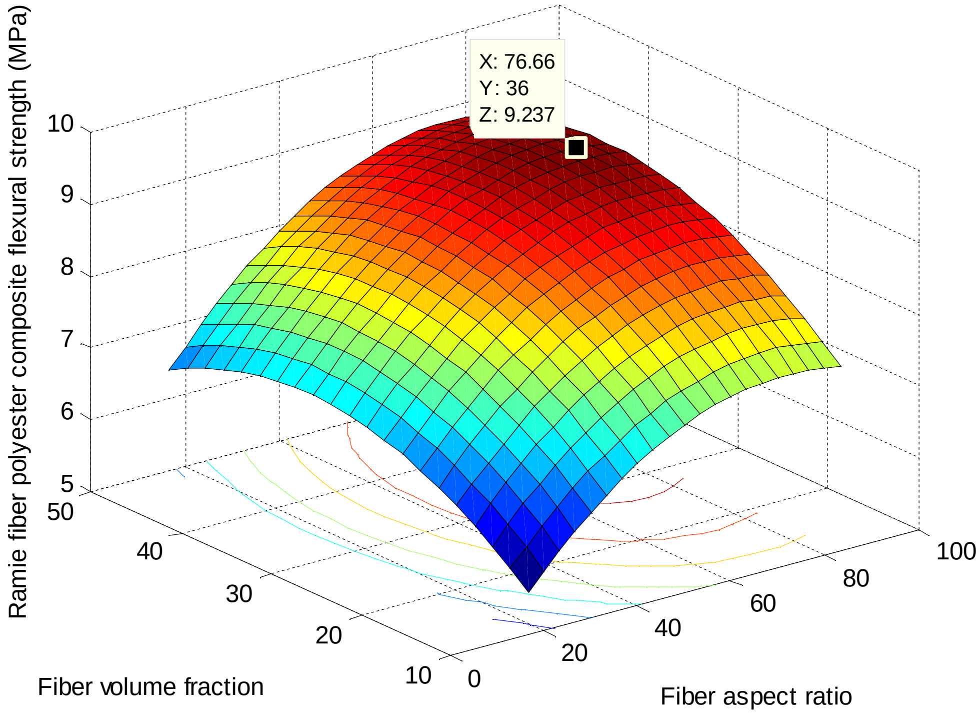

Fig.4: Surface plot for ramie fiber polyester Composite flexural strength

f. Optimization of ramie fiber polyester Composite flexural strength

Optimization terminated: first-order optimality measure less than options. TolFun and maximum constraint violation is less than options. TolCon.
No active inequalities.
x = 74.7759 36.3486
fval = -9.2395

g. Ramie fibre polyester composite ultrasonic pulse velocity

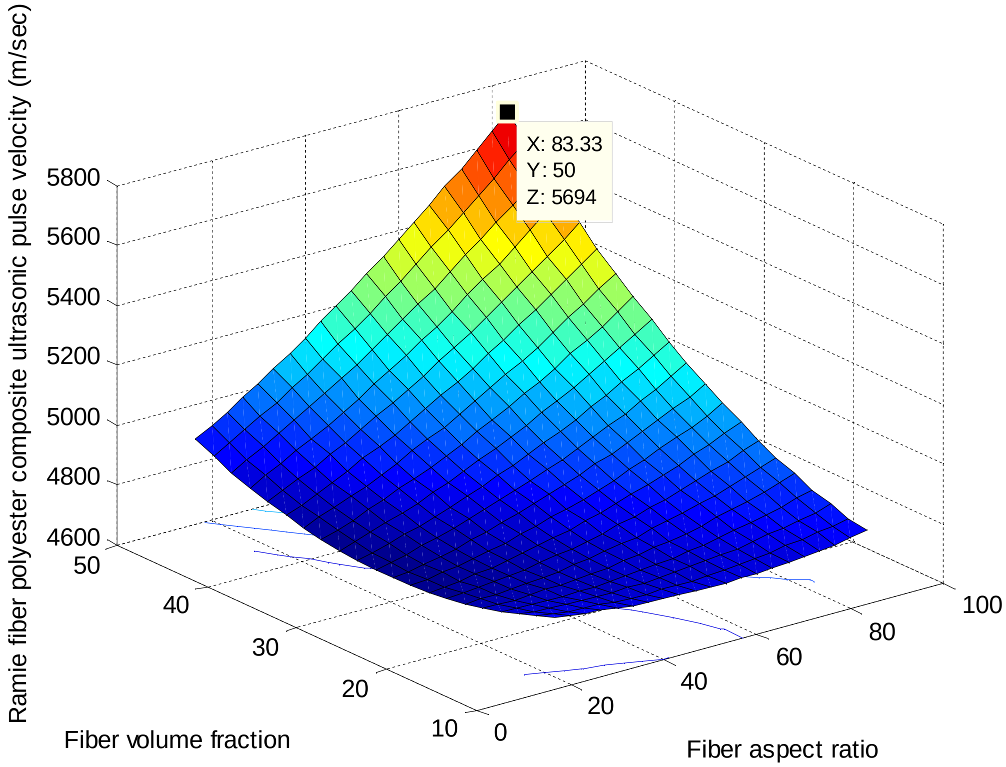

Fig.5: Surface plot for ramie fiber polyester Composite ultrasonic pulse velocity

h. Optimization of ramie fiber polyester Composite ultrasonic pulse velocity

Optimization terminated: first-order optimality measure less than options. TolFun and maximum constraint violation is less than options. TolCon.

Active inequalities (to within options.TolCon = 1e-006):

```
 lower     upper    ineqlin   ineqnonlin
             1          1
             2
x =   83.3300   50.0000
fval = -5.6940e+003
```

i. Regression models

Linear regression analyses in the form of models depicted in table 4 were employed to model the experimental results obtained.

Table 4: Individual composite strength linear regression analysis objective functions

Composite Strength properties	Regression models	R^2 %
Compressive strength	$Y = 39.73 + 0.28*(c_1) + 0.57*(c_2) - 0.001*(c_1c_2) - 0.002*(c_1^2) - 0.01*(c_2^2)$	91.53
Split tensile strength	$Y = 1.72 + 0.05*(c_1) + 0.08*(c_2) - 4.50e - 005*(c_1c_2) - 0.0002*(c_1^2) - 0.001*(c_2^2)$	99.39
Flexural trengsth	$Y = 2.84 + 0.10*(c_1) + 0.16*(c_2) + 0.0002*(c_1c_2) - 0.001*(c_1^2) - 0.002*(c_2^2)$	97.66
Ultrasonic pulse Velocity	$Y = 5109.50 - 7.04*(c_1) - 24.87*(c_2) + 0.30*(c_1c_2) + 0.04*(c_1^2) + 0.35*(c_2^2)$	81.93

where Y is predicted compressive strength, predicted split tensile strength, predicted Flexural strength, and predicted ultrasonic pulse velocity.

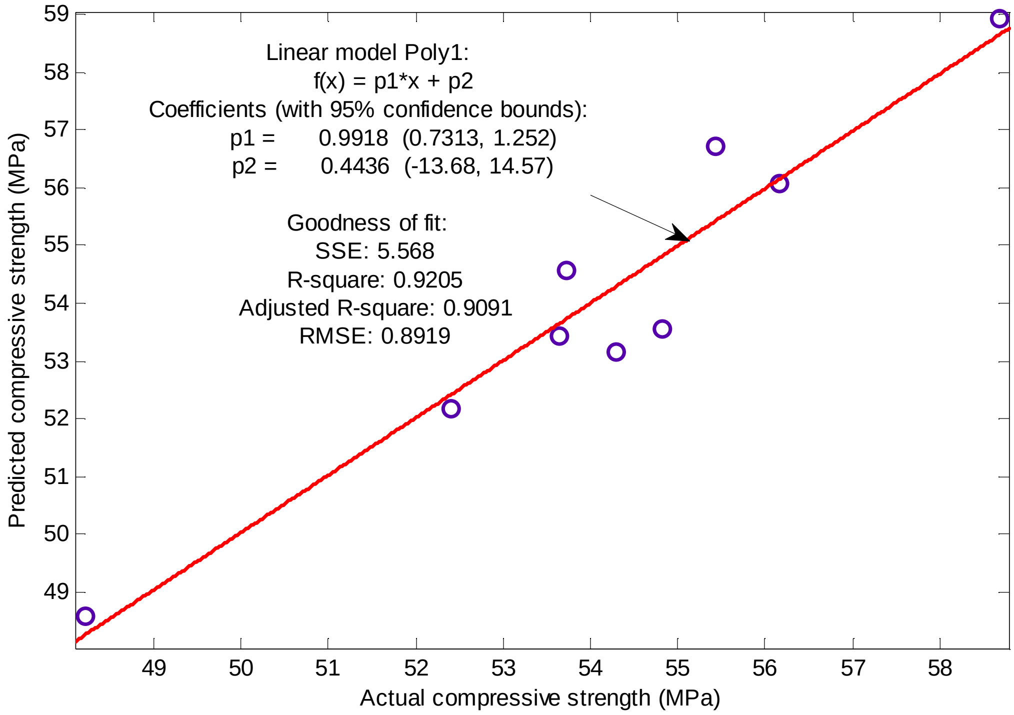

Fig.6: Fit for predicted vs. actual responses of composite compressive strength

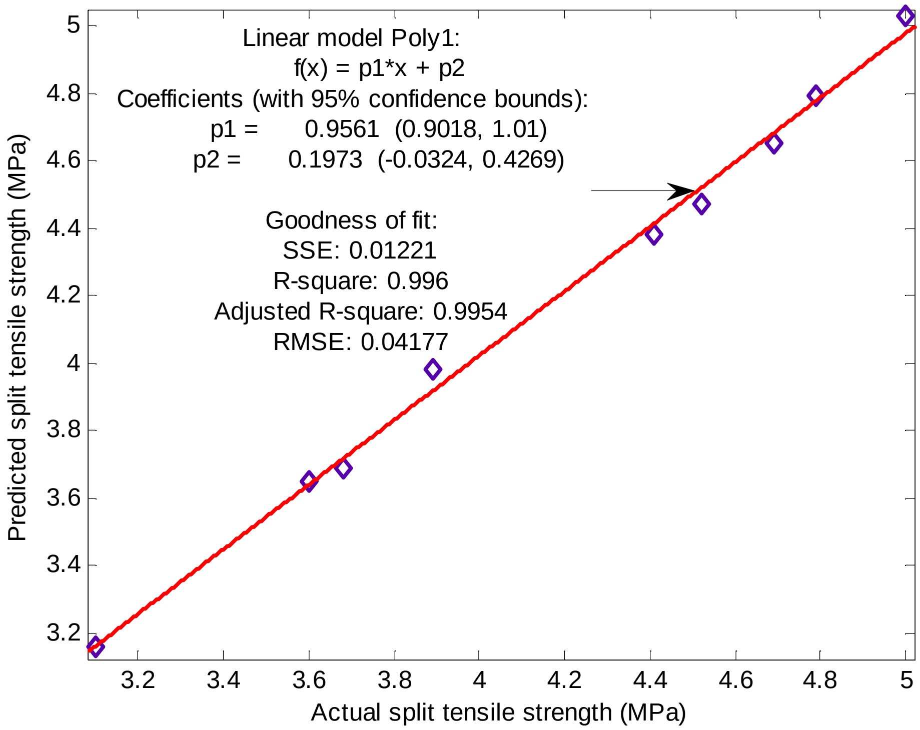

Fig.7: Fit for predicted vs. actual responses for composite split tensile strength

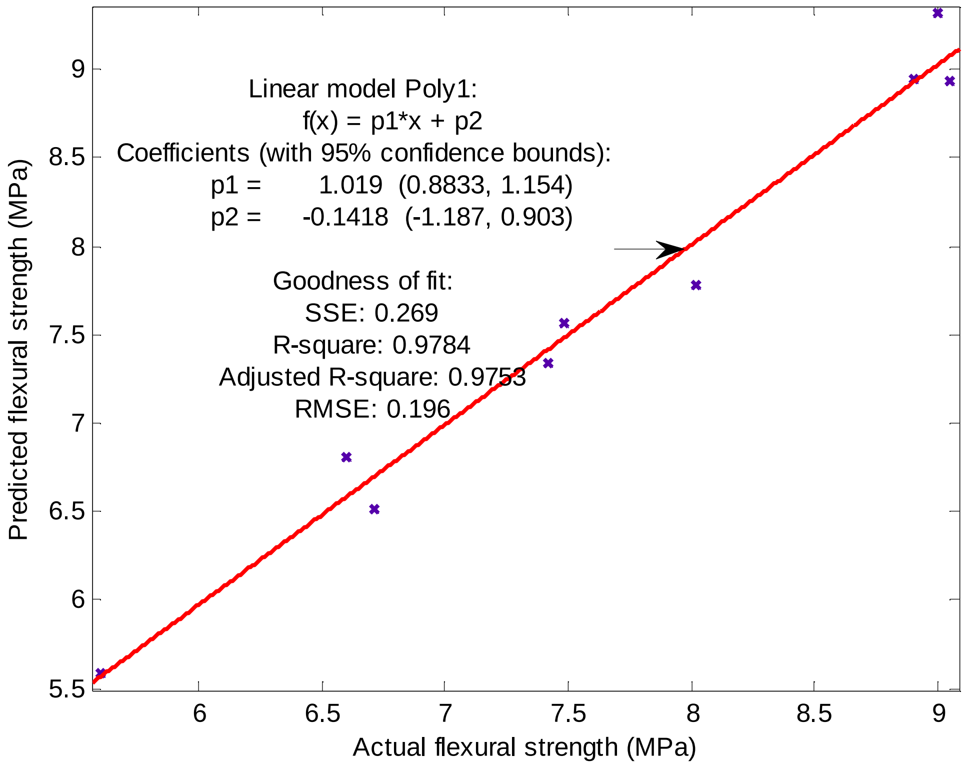

Fig.8: Fit for predicted vs. actual responses for composite flexural strength

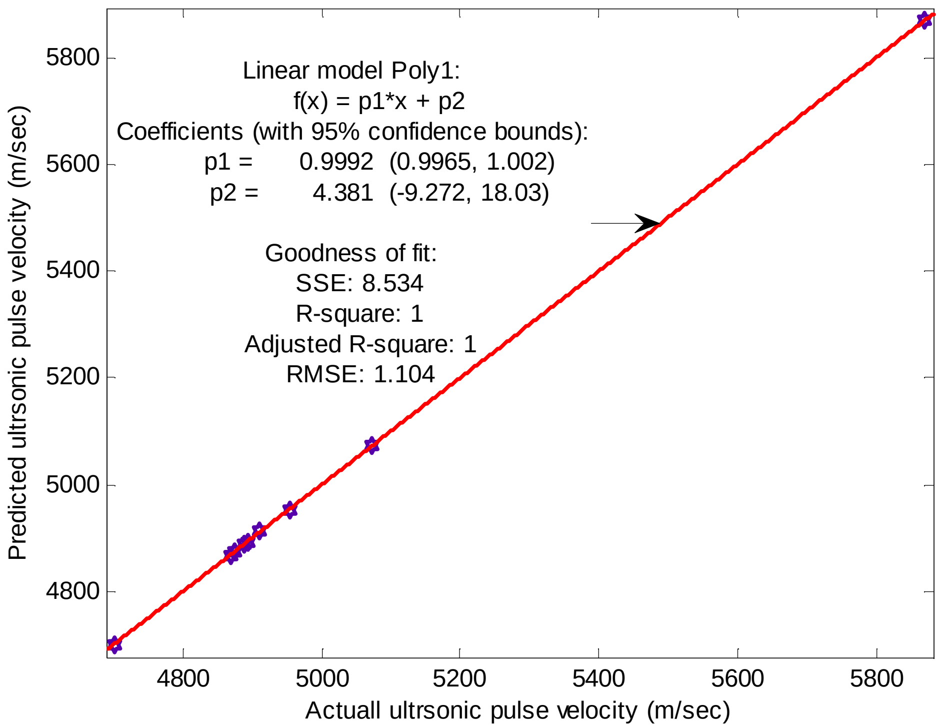

Fig.9: Fit for predicted vs. actual responses for composite ultrasonic pulse velocity

B. DISCUSSIONS

a. Fibre aspect ratio for the composite strength models

As observed from Table 3, the linear co-efficient of fibre aspect ratios for those of compressive strength model, split tensile strength model, flexural strength model were significant at 95 % significant confidence intervals with exception of ultrasonic pulse velocity model which was not significant at 95 % significant confidence intervals. As their individual magnitudes were two and above weather negative or positive. Their individual probability values ($pval$) shows that they are also significant at 95 % intervals because $pval \leq 0.05$ again with exception of ultrasonic pulse velocity model which was not significant at 95 % significant confidence intervals as it's $pval > 0.05$.

Also observed from Table 3, the quadratic co-efficient of fibre aspect ratios for those of compressive strength model, split tensile strength model, flexural strength model were significant at 95 % intervals with exception of ultrasonic pulse velocity model which was not significant at 95 % significant confidence intervals. As their individual magnitudes were two and above weather negative or positive. Their individual probability values ($pval$) shows that they are also significant at 95 % intervals because $pval \leq 0.05$ again with exception of ultrasonic pulse velocity model which was not significant at 95 % significant confidence intervals as it's $pval > 0.05$.

b. Fibre volume fraction for the composite strength models

As observed from Table 3, the linear co-efficient of fibre volume fractions for those of compressive strength model, split tensile strength model, flexural strength model were significant at 95 % intervals with exception of ultrasonic pulse velocity model which was not significant at 95 % significant intervals. As their individual magnitudes were two and above weather negative or positive. Their individual probability values ($pval$) shows that they are also significant at 95 % intervals because $pval \leq 0.05$ again with exception of ultrasonic pulse velocity model which was not significant at 95 % significant intervals as it's $pval > 0.05$.

Also observed from Table 3, the quadratic co-efficient of fiber volume fractions for those of compressive strength model, split tensile strength model, flexural strength model were significant at 95 % intervals with exception of ultrasonic pulse velocity model which was not significant at 95 % significant intervals. As their individual magnitudes were two and above weather negative or positive. Their individual probability values ($pval$) shows that they are also significant at 95 % significant intervals because $pval \leq 0.05$ again with exception of ultrasonic pulse velocity model which was not significant at 95 % intervals as it's $pval > 0.05$.

c. Compressive strength for the composite strength models

It was observed from Table 1 that the control composite mixture and composite reinforced with ramie fibre with various aspect ratios and volume fractions were depicted the strength study in it. The control polyester composite material compressive strength is 44.0 MPa. The ramie fibre aspect ratios of 16.67, 50.00 and 83.33 possess compressive strength of 48.2 MPa, 54.81 MPa and 58.68 MPa, respectively. Also depicted were the different mixture values of the composite samples. Compressive strength improved by 9.55 to 33.36 % as observed in Table 1 for ramie fibre reinforced with polyester polymer.

It was observed from Table 3 that the constant term, the coefficients of fibre aspect ratios and volume fractions, and their squares with the exception of their interactions all contributed to the changes at 95 % significant confidence intervals in composite compressive strength from the composite strength models. The accuracy of the model is 91.53 % at 95 % significant confidence interval with 58.03 MPa optimum composite compressive strength, 66.66 optimum fibre aspect ratio and 32 optimum fibre volume fraction as were observed from Figure 1 validated with those of the optimized parameters. Hence, the model was adequate at 95 % significant confidence bounds for fibre aspect ratio and adequate below 95 % significant confidence bounds for fibre volume fraction. Judging from probability values of ANOVA and F-stat in Table 2 which were able to explain 91.53 % varabilities in its modelled variables with the reduced form as: $y = \beta_0 + \beta_1 c_1 + \beta_2 c_2 + \beta_4 c_1^2 + \beta_5 c_2^2$.

It was observed from optimization of ramie fibre reinforced polyester polymer compressive strength at 95 % significant confidence interval. That optimum polyester polymer composite compressive strength was 58.0365 MPa (i.e., fval is the optimum response variable in this case polyester polymer composite compressive strength), optimum fibre aspect ratio as 66.9341 and optimum fibre volume fraction was also 32 (i.e., x is the optimum regressor variables, here were fibre aspect ratio and volume fraction).

As can be seen also from the output diagnostic messages, the feasibility of the solutions measured were not active absolute measures judging from constraint tolerance (TolCon) which is an upper bound for the constraint violation compared to the relative max (maximum constraint violation). Then, it depicted that x0 satisfies the constraints.

d. Split tensile strength for the composite strength models

It was observed from Table 1 also that the split tensile strength of all studied composite sample mixtures was represented. Its control polyester composite material split tensile strength is 2.6 MPa. Ramie aspect ratios of 16.67, 50.00 and to 83.33 possess split tensile strength of 3.1 MPa, 3.89 MPa and 5.00 MPa, respectively. Table 3 also depicts the percentage increase in split tensile strength values of ramie fibre reinforced polyester composite with various aspect ratios and there volume fractions. It is seen that split tensile strength of 19.23 to 92.31 % enhancements were obtained with ramie fibre reinforced polyester polymer composite. To utilize 50 % ramie fibre volume fractions seems to be promising as observed from Table 1.

It was observed from Table 3 that the constant term, the coefficients of fibre aspect ratios and volume fractions, and their squares with the exception of their interactions all contributed to the changes at 95 % significant intervals in composite split tensile strength from the composite strength models. The accuracy of the model is 99.39 % at 95 % significant confidence interval with 5.033 MPa optimum composite split tensile strength, 83.33 optimum fibre aspect ratio and 36 optimum fibre volume fraction as were observed from Figure 2 validated with those of the optimized parameters. Hence, the model was adequate at 95 % significant confidence bounds for both fibre aspect ratio and fibre volume fraction. Judging from probability values of ANOVA and F-stat in Table 2 which were was able to explain 99.39 % varabilities in its modelled variables with the reduced form as: $y = \beta_0 + \beta_1 c_1 + \beta_2 c_2 + \beta_4 c_1^2 + \beta_5 c_2^2$.

It was observed from optimization of ramie fibre reinforced polyester polymer split tensile strength at 95 % significant confidence interval. That optimum polyester polymer composite split tensile strength was 5.0337 MPa (i.e., fval is the optimum response variable in this case polyester polymer composite compressive strength), optimum fibre aspect ratio as 83.3300 and optimum fibre volume fraction was also 35.4734 (i.e., x is the optimum regressor variables, here were fibre aspect ratio and volume fraction).

As can be seen also from the output diagnostic messages, the feasibility of the solutions measured were active absolute measures judging from constraint tolerance (TolCon = 1e-006) which is an upper bound for the constraint violation compared to the relative max (maximum constraint violation). Then, it depicted that x0 satisfies the constraints.

e. Flexural strength for the composite strength models

Flexural strengths under current study were shown in Table 1 also. It is observed that its control composite flexural strength is 4.6 MPa. Ramie fibre with aspect ratios of 16.67, 50.00 and 83.33 possess flexural strength of 5.6 MPa, 7.42 MPa and 9.05 MPa, respectively. Ramie fibre addition increased flexural strength by 21.74 to 96.74 % as seen in Table1.

It was observed from Table 3 that the constant term, the coefficients of fibre aspect ratios and volume fractions, and their squares with the exception of their interactions all contributed to the changes at 95 % significant confidence intervals in composite flexural strength from the composite strength models. The accuracy of the model is 97.66 % at 95 % significant confidence interval with 9.237 MPa optimum composite flexural strength, 76.66 optimum fibre aspect ratio and 36 optimum fibre volume fraction as were observed from Figure 3 validated with those of the optimized parameters. Hence, the model was adequate at 95 % significant confidence bounds for both fibre aspect ratio and fibre volume fraction. Judging from probability values of ANOVA and F-stat in Table 2 which were able to explain 97.66 % varabilities in its modelled variables with the reduced form as: $y = \beta_0 + \beta_1 c_1 + \beta_2 c_2 + \beta_4 c_1^2 + \beta_5 c_2^2$.

It was observed from optimization of ramie fibre reinforced polyester polymer flexural strength at 95 % significant confidence interval. That optimum polyester polymer composite flexural strength was 9.2395 MPa (i.e., fval is the optimum response variable in this case polyester polymer composite flexural strength), optimum fibre aspect ratio as 74.7759 and optimum fibre volume fraction was also 36.3486 (i.e., x is the optimum regressor variables, here were fibre aspect ratio and volume fraction).

As can be seen also from the output diagnostic messages, the feasibility of the solutions measured were not active absolute measures judging from constraint tolerance (TolCon) which is an upper bound for the constraint violation compared to the relative max (maximum constraint violation). Then, it depicted that x0 satisfies the constraints.

f. Ultrasonic pulse velocity for the composite strength models

Average ultrasonic pulse velocity values for the samples were reported by Table 1 as observed. The control composite average ultrasonic pulse velocity is 4531 m/s. Ramie fibre reinforced polyester composite material with aspect ratios of 16.67, 50.00 and 83.33 possess average pulse velocity of 4700 m/s, 4875.25 m/s and 5870.65 m/s, respectively. The addition of ramie fibre has improved UPV by 3.73 –29.57 % seen from in Table 1.

It was observed from Table 3 that the coefficients of fibre aspect ratios and volume fractions, the coefficients of the squares of fibre aspect ratios and volume fractions, as well as the coefficients of their interactions with the exception of the constant term all did not contributed to the changes at 95 % significant confidence intervals but did below 95 % significant confidence intervals in composite ultrasonic pulse velocity from the composite strength models studied. The accuracy of the model is 81.93 % at 95 % significant confidence interval with 5694 m/sec optimum composite ultrasonic pulse velocity, 83.33 optimum fibre aspect ratio and 50 optimum fibre volume fraction as were observed from Fig.5 validated with those of the optimized parameters. Hence, the model was not adequate at 95 % significant confidence bounds but adequate below 95 % significant confidence intervals for both fibre aspect ratio and fibre volume fraction. Judging from probability values of ANOVA and F-stat in Table 2 which were able to explain 81.93 % varabilities in its modelled variables with the reduced form as$y = \beta_0 + \beta_2 c_2 + \beta_3 c_1 c_2 + \beta_5 c_2^2$.

It was observed from optimization of ramie fibre reinforced polyester polymer ultrasonic pulse velocity at 95 % significant confidence interval. That optimum polyester polymer composite ultrasonic pulse velocity was 5.6940e+003 m/sec (i.e., fval is the optimum response variable in this case polyester polymer composite ultrasonic pulse velocity), optimum fibre aspect ratio as 83.3300 and optimum fibre volume fraction was also 50.0000 (i.e., x is the optimum regressor variables, here were fibre aspect ratio and volume fraction).

As can be seen also from the output diagnostic messages, the feasibility of the solutions measured were active absolute measures judging from constraint tolerance (TolCon = 1e-006) which is an upper bound for the constraint violation compared to the relative max (maximum constraint violation). Then, it depicted that x0 satisfies the constraints.

g. Regression model for the composite strength models

Good associations between calculated/ experimental and predicted strength parameters were obtained as can be seen from Figs. 6, 7, 8, and 9.

IV. CONCLUSIONS

It was observed from Table 1 that the control composite mixture and composite reinforced with ramie fibre with various aspect ratios and volume fractions depicted the strength study in it. The control polyester composite material compressive strength is 44.0 MPa. The ramie fibre aspect ratios of 16.67, 50.00 and 83.33 possess compressive strength of 48.2 MPa, 54.81 MPa and 58.68 MPa, respectively. Also depicted were the different mixture values of the composite samples. Compressive strength improved by 9.55 to 33.36 % for ramie fibre reinforced with polyester polymer. Its control polyester composite material split tensile strength is 2.6 MPa. Ramie aspect ratios of 16.67, 50.00 and to 83.33 possess split tensile strength of 3.1 MPa, 3.89 MPa and 5.00 MPa, respectively.

Table 3 also depicts the percentage increase in split tensile strength values of ramie fibre reinforced polyester composite with various aspect ratios and there volume fractions. It is seen that split tensile strength of 19.23 to

92.31 % enhancements were obtained with ramie fibre reinforced polyester polymer composite. To utilize 50 % ramie fibre volume fractions seems to be promising as observed from Table 1. It is observed that its control composite flexural strength is 4.6 MPa. Ramie fibre with aspect ratios of 16.67, 50.00 and 83.33 possess flexural strength of 5.6 MPa, 7.42 MPa and 9.05 MPa, respectively. Ramie fibre addition increased flexural strength by 21.74 to 96.74 % as seen in Table1.The control composite average ultrasonic pulse velocity is 4531 m/s. Ramie fibre reinforced polyester composite material with aspect ratios of 16.67, 50.00 and 83.33 possess average pulse velocity of 4700 m/s, 4875.25 m/s and 5870.65 m/s, respectively. The addition of ramie fibre has improved UPV by 3.73 –29.57 % seen from in Table 1.

Also, from strength properties models it is found that the ramie fibre polyester polymer composites has optimum compressive strength of 58.03 MPa at 95 % adequacies with 66.66 optimum fibre aspect ratio and 32 optimum fibre volume fraction at 91.53 % accuracy all at 1.8500 mean square error. Also, 5.033 MPa and 9.237 MPa, optimum split tensile and flexural strengths at 95 % adequacies with 83.33 and76.66 optimum fibre aspect ratios and 36 optimum fibre volume fractions at 99.39 % and 97.66 % accuracies all at 0.0067 and 0.0918 mean square errors. Then, that of optimum ultrasonic pulse velocity is 5694 m/sec below 95 % adequacies with 83.33 optimum fibre aspect ratio and 50 optimum fibre volume fraction at 81.93 % accuracy all at 5.5369e+04 mean square error.

Conflict of interest

The authors declare that there is no conflicting interest in the publication of this paper.

Acknowledgments

The authors will like to acknowledge the HND II chemical engineering final year students of chemical engineering technology department of Federal Polytechnic Nekede, Owerri, Imo State, Nigeria. Final year students of chemical engineering department of Micheal Okpara University of Agriculture, Umudike, Abia State, Nigeria for the finance of experiments needed for the outcome of this publication.

REFERENCES

Abedom, F., Sakthivel, S., Asfaw, D., Melese, B., Solomon, E., Kumar, S. S. (2021). Development of Natural Fiber Hybrid Composites Using Sugarcane Bagasse and Bamboo Charcoal for Automotive Thermal Insulation Materials. Adv. Mater. Sci. Eng. 2021, 2508840.

Alhazmi, W. H., Jazaa, Y., Mousa, S., Abd-Elhady, A. A., Sallam, H. E. M. (2021). Tribological and Mechanical Properties of Epoxy Reinforced by Hybrid Nanoparticles. Lat. Am. J. Solids Struct. 18, e361.

Chokshi, S., Parmar, V., Gohil, P., Chaudhary, V. (2020). Chemical Composition and Mechanical Properties of Natural Fibers. J. Nat. Fibers 17, 1–12.

Dungani, R., Karina, M., Subyakto, Sulaeman, A., Hermawan, D., Hadiyane, A. (2016). Review Article Agricultural Waste Fibers Towards Sustainability and Advanced Utilization: A Review. Asian J. Plant Sci. 15, 42–55.

Ezeokpube, G.E., Mbadike, E., Okoronkwo, G. O., Onukwuli, O. D. (2018). The effect of fibre hydro-expansion on the tensile property of wire weed fibre. Umudike Journal of Engineering and Technology, Volume 4, Number 3, 12 – 19.

Ezeokupbe, G. E., Okoronkwo, G. O., Oraegbune, M. O., Onukwuli, O. D. (2018). Modeling liquid water absorption of finger root fibre during soaking. Umudike Journal of Engineering and Technology, Volume 4, Number 3, 163 – 19167.

Ezeokpube, G. E., Okoronkwo G. O., Madappa V. R. Sivasubramanian. (2019). Effects Of Strength Properties On Sisal-Fique-Areca Fibers-Reinforced Thermoset-Hybrid Composite Materials. *Oriental Journal of Science & Engineering VOL -1, ISS-1.*

Ezeokpube, G. E., Okoronkwo G. O., Madappa, V. R. Sivasubramanian. (2019). Micro-Hybridization Modelling and Analysis of Tensile and Flexural Strengths of Hybrid Bamboo-Coconut Reinforced Thermoset Composite Materials. *Oriental Journal of Science & Engineering VOL -1, ISS-1.*

Ferdous, W., Ngo, T. D., Nguyen, K. T. Q., Ghazlan, A., Mendis, P., Manalo, A. (2018). Effect of fire-retardant ceram powder on the properties of phenolic-based GFRP composites. Compos. Part B Eng. 155, 414–424.

Ferdous,W., Manalo, A., AlAjarmeh, O., Mohammed, A. A., Salih, C., Yu, P., Khotbehsara, M. M., Schubel, P. (2021). Static behaviour of glass fibre reinforced novel composite sleepers for mainline railway track. Eng. Struct. 229, 111627.

Karimah, A., Ridho, M. R., Munawar, S. S., Adi, D. S., Ismadi, Damayanti, R., Subiyanto, B., Fatriasari, W., Fudholi, A. (2021). A review on natural fibers for development of eco-friendly bio-composite: Characteristics, and utilizations. J. Mater. Res. Technol. 13, 2442–2458.

Kumar, R., Bhowmik, S. (2019). Elucidating the Coir Particle Filler Interaction in Epoxy Polymer Composites at Low Strain Rate. Fibers Polym. 20, 428–439.

Madu, K. E., Nwankwo, E. I., Okoronkwo, G. O., Onyewudiala, J.I. (2020). Investigative Analysis of the Tensile and Impact Strengths of Hybridized Aluminum Metal Matrix Composite Materials. Journal of Scientific Research and Reports, 26(3): 72 – 79.

Madu, K. E., Nwankwo, E. I., Okoronkwo, G. O., Onyewudiala, J.I. (2019). Micro-Mechanics Mercerization Analysis on the Tensile Strength and Interphase Quality of Stipa Stem Fibre-Reinforced Polypropylene Composite Materials. Iconic Research and Engineering Journals, Volume 3, Issue 5: 73 – 88.

Madu, K. E., Okoronkwo, G. O. (2018). Analysis of adsorptive treatment of Brewery Effluent with Activated Black Date Seed Carbon. Equatorial Journal of Engineering, 78 – 84.

Madu, K. E., Okoronkwo, G. O. (2018). Analysis of adsorptive treatment of Brewery Effluent with Activated Black Date Seed Carbon. Equatorial Journal of Engineering, 78 – 84.

Madu, K. E., Okoronkwo, G. O. (2018). Damage and failure effects on residual stresses analysis of areca fibre reinforced epoxy polymer composite materials. Journal of Polymer Research, pg 1 – 9.

Madu, K. E., Okoronkwo, G. O. (2018). Epoxy composites reinforced with natural chicken fibres obtained from livestock feathers. Research in Material Science, pg 16 – 23.

Madu, K. E., Okoronkwo, G. O. (2018). Hybridization analysis of ramie-glass fibre reinforced metal composite laminates tensile and fatigue strengths. Journal of Polymer Research, 1 (1): 10 – 15.

Madu, K. E., Okoronkwo, G. O. (2018). Structural and micro-strength analysis and modelling of natural ukam fibre reinforced epoxy viscoelastic laminated composite plates. Equatorial Journal of Computational and Theoretical Science, 2 (2): 21 – 30.

Madu, K. E., Okoronkwo, G. O., Nwankwo, E. I. (2019). Analysis of Fique Fibre Thermo-set Vinyl-ester composite Flexural Strengtrhs: international Journal of Latest Engineering and Management Research, Volume 04; Issue 06: Pp 60 – 66.

Madu, K. E., Okoronkwo, G. O., Orji, M. E.K. (2019). Analysis of Areca Plant Stem Fibre Reinforced Polyester Thermo-set Composite Mechanical Properties. International Journal of Engineering and Technical Research, Volume - 9; Issue - 8: 28 – 32.

Messana, A., Airale, A. G., Ferraris, A., Sisca, L., Carello, M. (2017). Correlation between thermo-mechanical properties and chemical composition of aged thermoplastic and thermosetting fiber reinforced plastic materials. Mater. Werkst. 48, 447–455.

Mochane, M.J., Mokhena, T. C., Mokhothu, T. H., Mtibe, A., Sadiku, E. R., Ray, S. S., Ibrahim, I. D., Daramola, O. O. (2019). Recent progress on natural fiber hybrid composites for advanced applications: A review. Express Polym. Lett. 13, 159–198.

Moudood, A., Rahman, A., Huq, N. M. L., Öchsner, A., Islam, M. M., Francucci, G. (2020). Mechanical properties of flax fiber-reinforced composites at different relative humidities: Experimental, geometric, and displacement potential function approaches. Polym. Compos. 41, 4963–4973.

Neves, A. C. C., Rohen, L. A., Mantovani, D. P., Carvalho, J. P. R. G., Vieira, C. M. F., Lopes, F. P. D., Simonassi, N. T., da Luz, F. S., Monteiro, S. N. (2020). Comparative mechanical properties between biocomposites of Epoxy and polyester matrices reinforced by hemp fiber. J. Mater. Res. Technol. 9, 1296–1304.

Okoronkwo G. O., Ifegbo, A. N. (2019). The Effects of Regressors on Tensile Strength Responses of Rhus Fiber Reinforced Thermo-set Composites. *Oriental Journal of Science & Engineering VOL -2, ISS-1.*

Okoronkwo, G. O., Madu, K. E., Nwankwo, E. I. (2019). Effects of Fibre Volume Fraction and Curing Time on Impact – Hardness Strength Properties of Areca Fibres Reinforced Polyester Thermo-set Composites: Research Journal of Mechanical Operations, Volume 1; No. (2): Page(s) 31 – 37.

Okoronkwo, G. O., Madumelu, P. C. (2016). Chemical treatment of natural areca fibre for use in natural fibre reinforced composites. International Journal of Innovative Engineering, Technology and Science, Vol. 1, no. 2, pg 101 – 105.

Onukwuli, O. D., Okoronkwo, G. O. (2016). Tensile properties of ramie fibre reinforced epoxy composites. International Journal of Innovative Engineering, Technology and Science, Vol. 1, no. 2, pg 220 – 225.

Othman, H., Marzouk, H. (2016). Strain Rate Sensitivity of Fiber-Reinforced Cementitious Composites. ACI Mater. J. 113, 143–150.

Riccio, A., Raimondo, A., Saputo, S., Sellitto, A., Battaglia, M., Petrone, G. (2018). A numerical study on the impact behaviour of natural fibres made honeycomb cores. Compos. Struct. 202, 909–916.

Sanjay, M. R., Madhu, P., Jawaid, M., Senthamaraikannan, P., Senthil, S., Pradeep, S. (2018). Characterization and properties of natural fiber polymer composites: A comprehensive review. J. Clean. Prod. 172, 566–581.

Sharavanan, R. (2018). A Review on Natural Fiber Hybrid Composites. Int. J. Mech. Prod. Eng. Res. Dev. 943–948.

Silva, M. P., Santos, P., Sousa, N. N., Reis, P. N. B. (2019). Strain rate effect on composites with epoxy matrix filled by cork powder. Mater. Des. Process. Commun. 1, 1–9.

Wang, X., Xie, J., Zhang, H., Zhang, W., An, S., Chen, S., Luo, C. (2019). Determining the lignin distribution in plant fiber cell walls based on chemical and biological methods. Cellulose 26, 4241–4252.